Enhancing Humidity Resistance of Nickel-rich Layered Cathode Materials by Low Water-soluble CaF$_2$ Coating

Zijian Zhang [a], Jiajin Feng [a], Ran He [a], Yelong Zhang [a], Hangmin Zhu [a], Feng Wu [a],

Qingguang Zeng [a], Hui Yu [b], Kwun Nam Hui [c], Xi Liu [*b] and Da Wang [*a]

[a]School of Applied Physics and Materials, Wuyi University, Jiangmen 529020, China

[b]Guangdong-Hong Kong Joint Laboratory for New Textile Materials, School of Textile Materials and Engineering, Wuyi University, Jiangmen 529020, China

[c]Joint Key Laboratory of the Ministry of Education, Institute of Applied Physics and Materials Engineering, University of Macau, Avenida da Universidade, Taipa, Macau

*Corresponding Author: dawang@mail.ustc.edu.cn (D. W.); liuxi@wyu.edu.cn (X. L.)

Experimental Section

Materials Preparation

CaF$_2$@NMC811 samples were prepared using two step reactions including hydroxide co-precipitation and the gas-phase reaction. Initially, CaCl$_2$ (3 mg, 6 mg, and 9 mg) was dissolved in ethanol solvent. The solution was then subjected to ultrasonic

dispersion for 1 hour at room temperature, 0.2 g of NMC811 (Hefei Kejing Co.) powder was added to the solution, followed by 5 minutes of ultrasonic dispersion and 30 minutes of stirring. Subsequently, a 1 ml 0.1 mol/L LiOH aqueous solution was slowly added dropwise with magnetic stirring, and the mixture was stirred for an additional 30 minutes. After the co-precipitation step, the precipitate was centrifuged and rinsed three times with water to remove any residual LiOH and dried at 80°C for 2 hours. The dried samples were then gathered and placed inside a quartz boat, which was subsequently inserted into a tube furnace. The temperature was gradually increased at a rate of 5 °C per minute, while a continuous flow of O_2 was maintained until it reached 300 °C, at which, the gas was switched to NF_3 (Yuejia Gas Co. 95% Ar and 5% NF_3) and held steady for 3 minutes. Subsequently, the gas flow was reverted back to O_2, and the samples were left to undergo a natural annealing process, resulting in the final samples (1.5%, 3.0% and 4.5% in weight) CaF_2@NMC811. For 3.0% CaF_2@NMC811-Crystal, the 3.0% CaF_2@NMC811 sample was placed within a crucible and then introduced into a muffle furnace. The temperature within the furnace was raised at a rate of 10 °C per minute until it reached 500 °C, where it was held for a duration of 6 hours. NF_3@NMC811 sample was made through NF_3 fluorination reaction without the first precipitation step of introducing Ca ions. The untreated NMC811 and 3.0% CaF_2@NMC811 samples were subjected to storage in a humid environment (RH >85%) for 7 days for moisture susceptibility comparison. For water exposure test, 100 mg of sample was introduced into 5 ml of deionized water and then subjected to continuous stirring at a speed of 800 r/min for 15 minutes,

followed by 5 min settling, allowing suspended particles to precipitate. The precipitated sample was then dried at 80°C for 10 hours before further analysis.

Cathode fabrication, coin cell assembly and electrochemical test

The pellet cathode electrode is composed of a mixture of 80% active materials 10% Super P carbon (SP), and 10% poly vinylene difluoride (PVDF) binder. The mixing process was conducted using a conventional mortar and pestle, during which active material, SP and PVDF were added to the mortar in sequence and ground for 20 min. The mixture was poured into a 13 mm tablet mold and pressed into small pellets. Each pellet cathode electrode weighs about 4~5 mg. The casting electrodes were made through the conventional doctor blade method. For the electrodes processed with NMP, cathode slurries contained 80 wt% active materials, 10 wt% SP, and 10 wt% binder (PVDF); for electrodes processed aqueously, slurries contained 80 wt% active materials, 10 wt% SP, 3 wt% carboxymethylcellulose (CMC) and 7 wt% Styrene Butadiene Rubber (SBR) emulsion. Each casting cathode electrode weighs about 2~3 mg. All the electrodes were dried at 80 °C in a vacuum oven for over 8 h before assembling coin-type cells in an argon-filled glovebox. The coin cells were composed of a cathode electrode, a Celgard 2500 separator, a Li-metal anode, and the LB-001 electrolyte (1M $LiPF_6$ in EC/DMC=1:1 vol%, Suzhou DuoDuo Chemical Technology Co. Ltd). The coin cells were cycled at 0.1 C charge-discharge rate for three cycles and at 0.5 C afterwards. Galvanostatic charge-discharge cycling tests were carried out on battery cyclers (CT3001A LAND). The Electrochemical Impedance Spectroscopy

(EIS) was measured on VMP3 electrochemical workstation with a frequency range from 100 kHz to 0.1 Hz.

Characterization

X-ray Photoelectron Spectroscopy (XPS) was tested through 150 W monochromatic Al Kα radiation (hν = 1486.6 eV) at the high voltage of 12 kV by Thermo Fisher Nexsa. The charge offset was performed by correcting the standard peak C 1s peak of the contaminated carbon at 284.8 eV. Fourier Transform Infrared Spectrometer (FTIR) was used to analysis surface chemistry of the sample by VER TEX 70 (Bruker). X-ray Diffraction (XRD) was conducted for the pristine and coated NMC811 samples with Cu Kα radiation (λ = 1.54056 Å) at a 2θ range of 10° ~ 80° by SmartLab 9kw. Scanning Electron Microscope (SEM) was used to characterize the particle morphology of the samples by ZEISS SEM Gemini 300 and Energy Dispersive Spectroscopy (EDS) was used to characterize the elemental mapping distribution of the samples by Oxford X-Max. Transmission Electron Microscope (TEM) images were obtained by characterization with a transmission electron microscope (JEOL JEM 2100). The pH value of the remaining solutions after water exposure test was measured by a pH meter (PH-20, MITR). The wetting angle test was conducted on the DSA-X ROLL instrument.

Table S1. Potential compounds and their solubility in water at 20 °C.

Compound	Solubility (g/100 cm³)	Compound	Solubility (g/100 cm³)
CaF_2	1.56×10^{-2}	AgCl	1.92×10^{-4}
SrF_2	3.90×10^{-3}	AgBr	1.33×10^{-5}
CuF_2	7.50×10^{-2}	$CaCO_3$	7.00×10^{-4}
FeF_3	9.10×10^{-2}	$BaCO_3$	1.40×10^{-3}
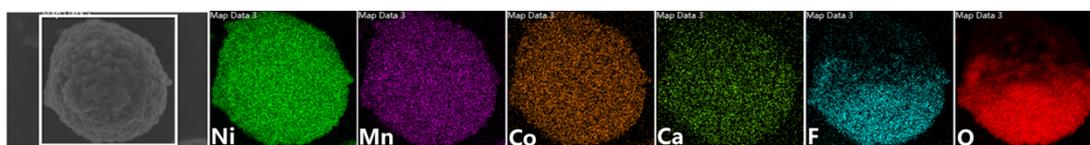
Fig. S1. EDS mapping of Ni, Mn, Co, Ca, F and O for 3.0% CaF_2@NMC811, respectively.
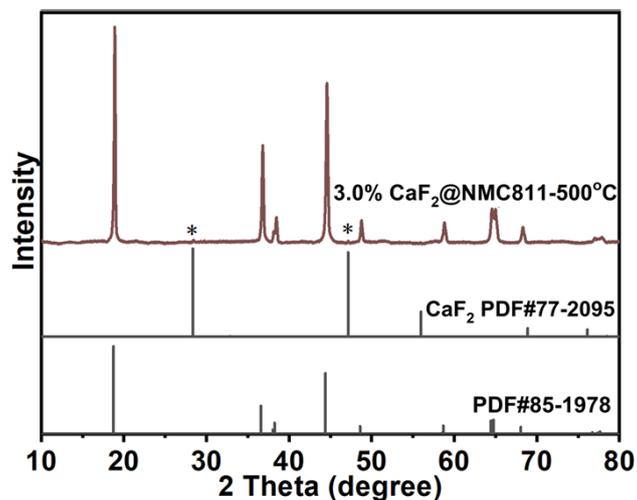
Fig. S2. XRD patterns of 3.0% CaF_2@NMC811 samples after higher temperature (500 °C) calcination, CaF_2 indicated by asterisks, corresponding to PDF#77-2095. Tiny peaks of CaF_2 can be clearly seen if 500 °C calcination, suggesting CaF_2 exists as an amorphous form for calcination at a lower temperature, 300 °C.
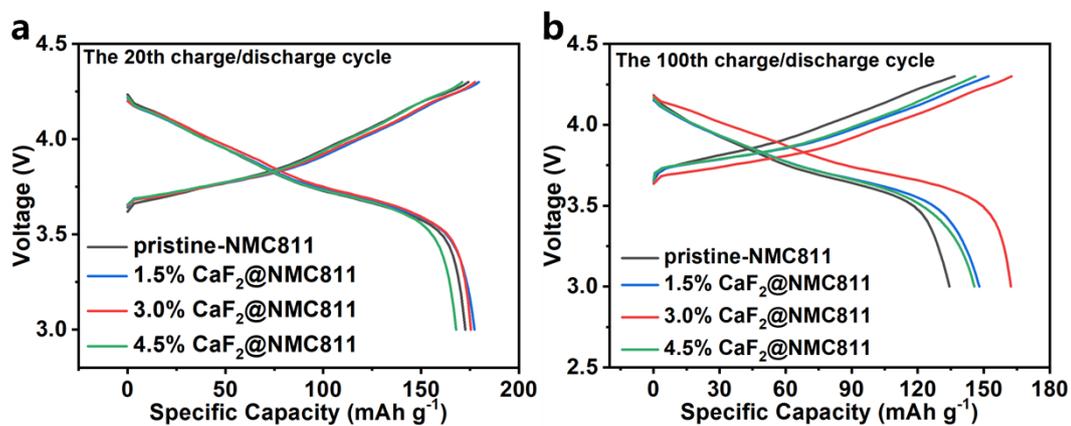

Fig. S3. The (a) 20th and (b) 100th charge-discharge curves of pristine-NMC811 and CaF_2@NMC811 samples with different coating levels in the voltage range of 4.3-3.0 V at room temperature at 0.5 C. 3.0% CaF2@NMC811 sample has the best capacity retention.

The impedance of the samples increases with the levels of CaF_2 after the first cycle (Figure S4a), which is due to the relatively poor electrical conductivity of CaF_2. However, the impedance of 3.0% CaF_2@NMC811 became smaller than that of pristine-NMC811, after several cycles (Figure S4b, c).
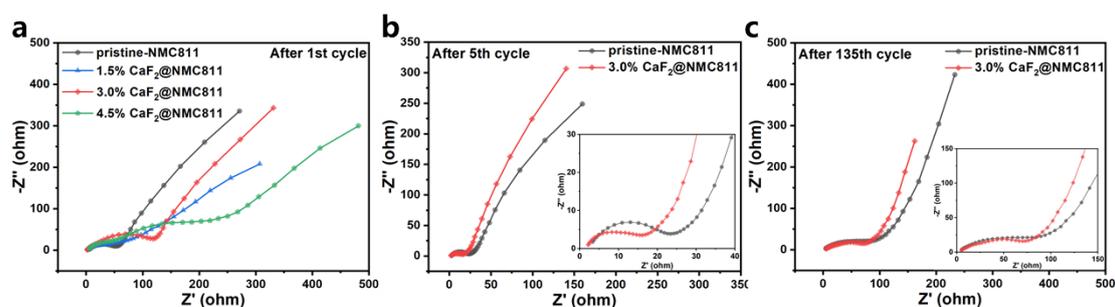

Fig. S4. (a) EIS Nyquist plots of pristine-NMC811 and CaF_2 coated NMC811 with levels of 1.5%, 3.0% and 4.5% after the 1st cycle. EIS Nyquist plots of pristine-NMC811 and 3.0% CaF_2@NMC811 after (b) the 5th cycle and (c) 135th cycle, confirming the cell with 3.0% CaF_2@NMC811 has lower impedance after cycles.
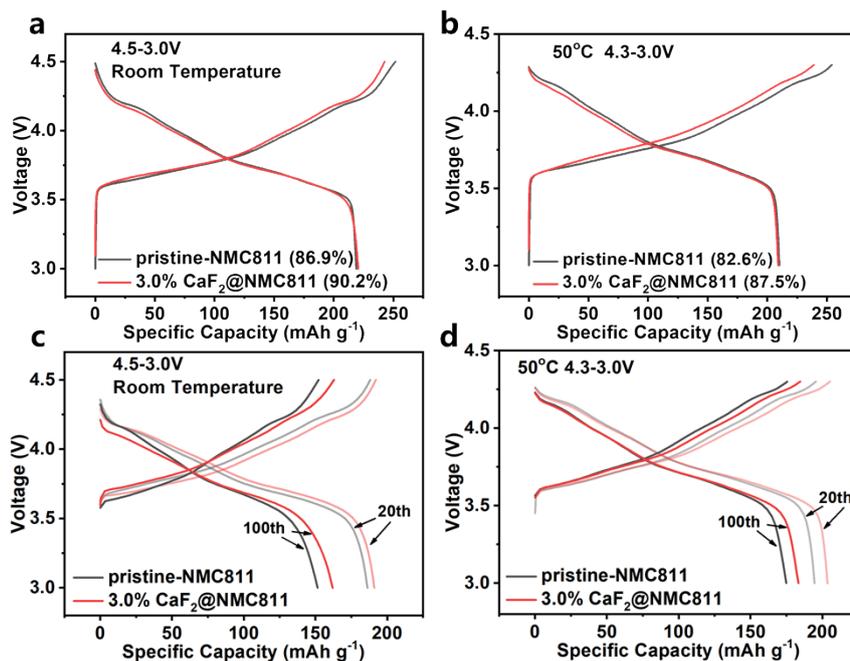
Fig. S5. Charge-discharge curves of pristine-NMC811 and 3.0% CaF$_2$@NMC811 samples, the first cycle at 0.1 C (a) and (b), the 20th and 100th cycles at 0.5 C (c) and (d).
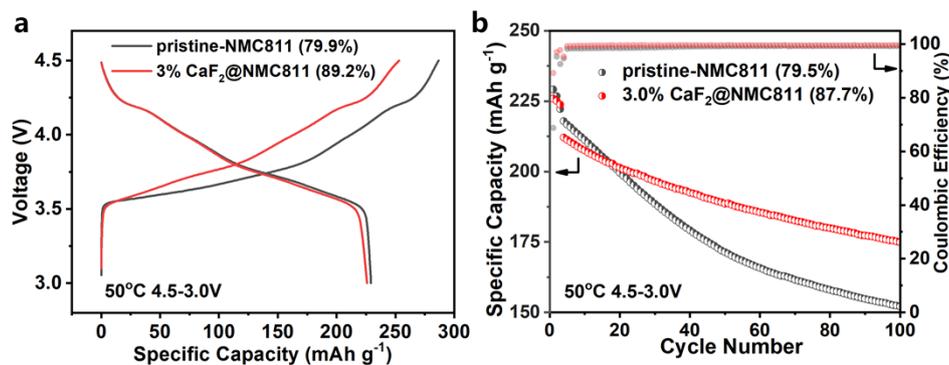

Fig. S6. Electrochemical performance of pristine-NMC811 and 3.0% CaF$_2$@NMC811 samples in the voltage range of 4.5-3.0 V at 50 °C (a) initial charge-discharge curves with CE at 0.1 C rate and (b) cycling performance and coulombic efficiency at 0.1 C in the first three cycles and 0.5 C afterwards.

Either at higher charge voltage or elevated temperature, Fig. S5 or at both conditions Fig. S6, 3.0% CaF$_2$@NMC811 has better electrochemical performance than pristine one.
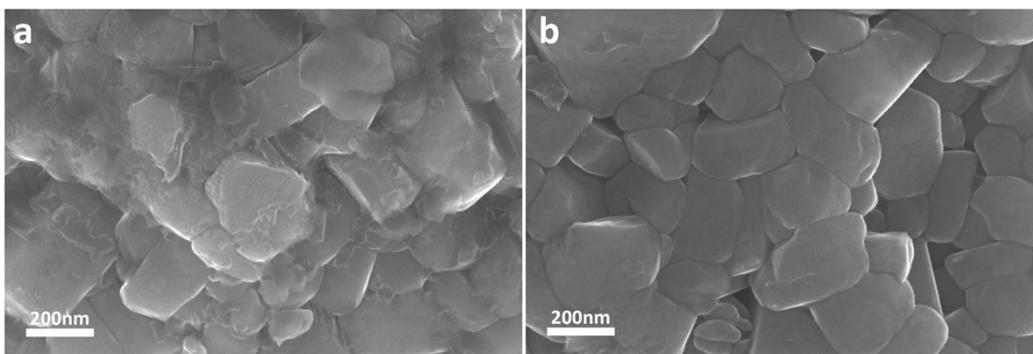
Fig. S7. SEM images of (a) pristine-NMC811 and (b) 3.0% CaF$_2$@NMC811 samples stored under moist environment (humidity > 85%) for 7 days.
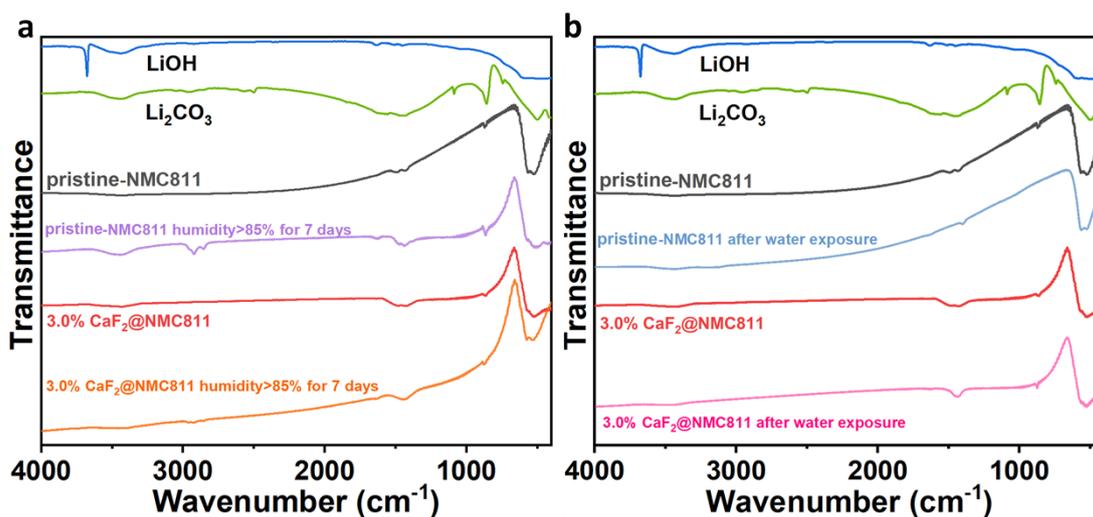

Fig. S8. FTIR spectra of NMC811 and 3.0% CaF$_2$@NMC811 samples (a) before and after storage under moist environment (humidity > 85%) for 7 days and (b) before and after water exposure. The spectra of LiOH and Li$_2$CO$_3$ are put here for reference.
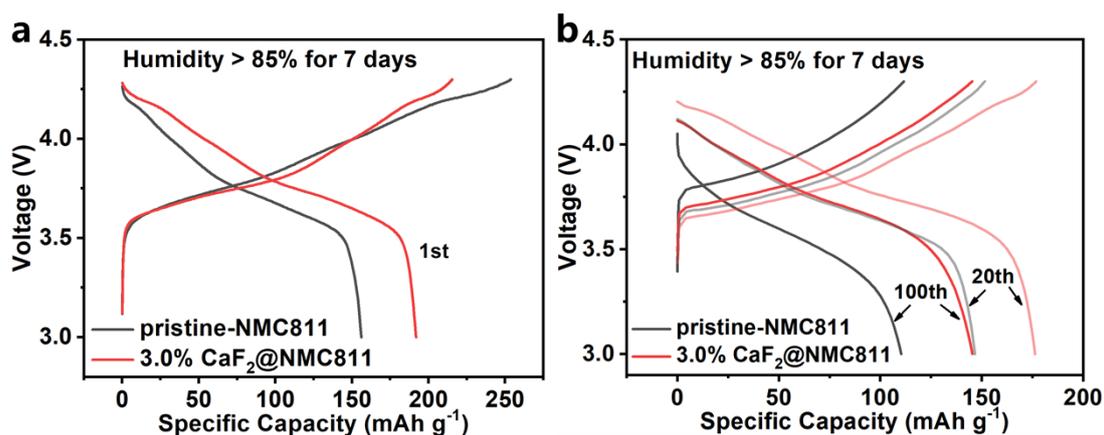
Fig. S9. The first at 0.1 C (a), 20th and 100th cycle at 0.5 C (b), charge-discharge curves of pristine-NMC811 and 3.0% CaF$_2$@NMC811 samples stored under moist environment (humidity > 85%) for 7 days.
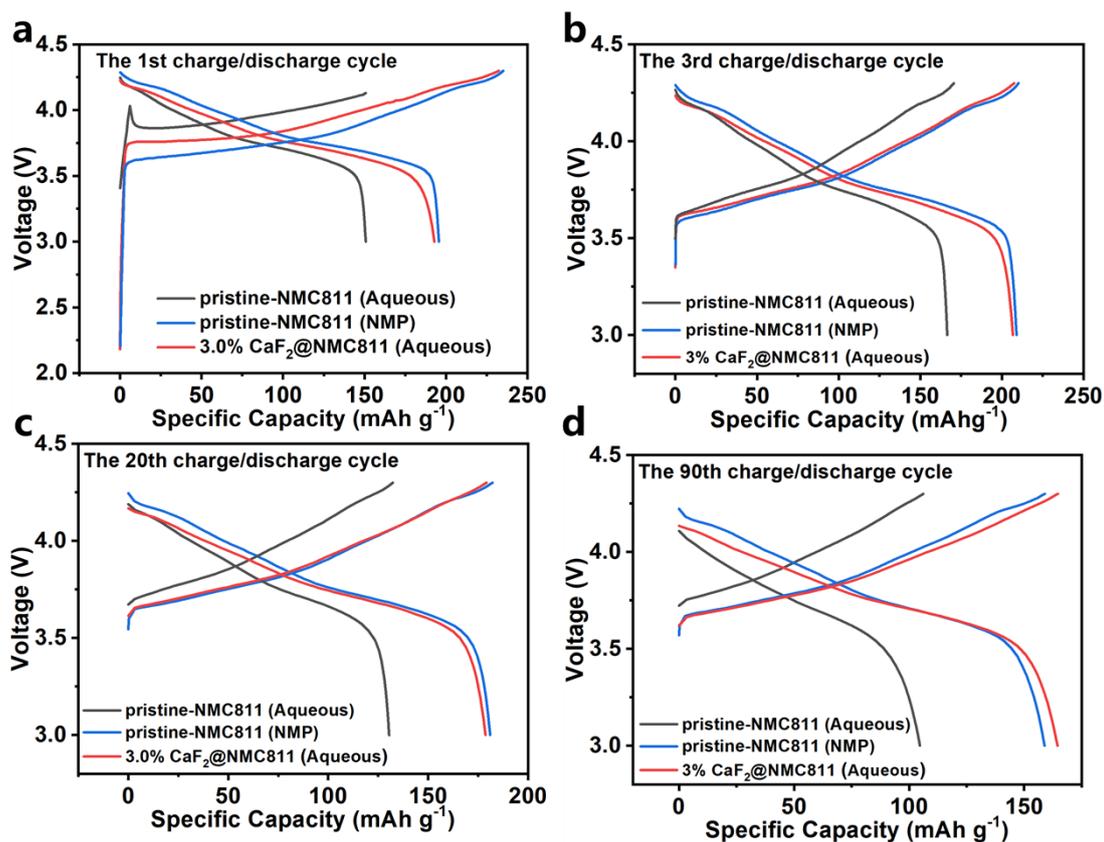

Fig. S10. The first (a) and 3rd (b) at 0.1 C, 20th (c) and 90th cycle (d) at 0.5 C, charge-discharge curves of pristine-NMC811 and 3.0% CaF$_2$@NMC811 electrodes prepared through aqueous and NMP routes.
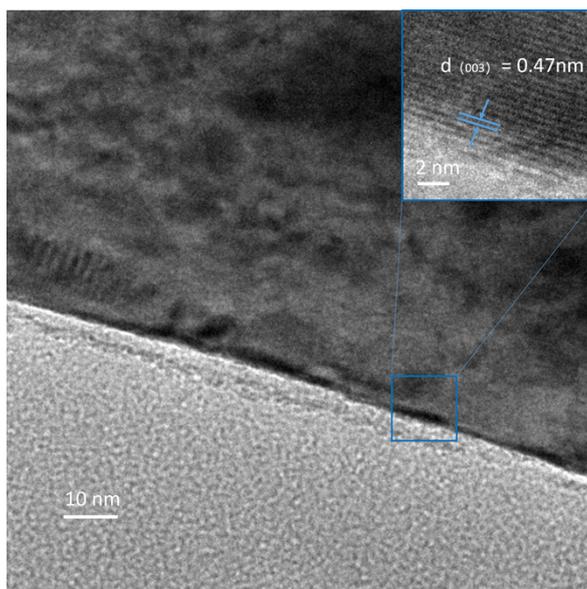
Fig. S11. TEM image of the 3.0% CaF_2@NMC811 sample after water exposure, demonstrating the lattice of the sample keeps intact, the lattice spacing of (003) is 0.47 nm, consistent with the XRD result.

The O–H signal associated with pristine-NMC811, observed at 531.0 eV, exhibits a significant enhancement after water exposure, as depicted in Fig. S12a. However, the Ni^{3+} percentage remains unchanged for the 3.0% CaF_2@NMC811 sample (Fig. 4c). The slight increase in the O–H signal (Fig. S13a) may be attributed to a few residual lithium compounds still generated on the surface of the CaF_2 protective layer. This suggests that NMC811 particles may not be entirely covered by CaF_2, consistent with the electrochemical performance of water-based electrode. Furthermore, the characteristic Li_2CO_3 peak, located near 289.3 eV for the pristine-NMC811 sample, diminishes after water exposure, indicating that water effectively removes residual lithium carbonate compounds, as demonstrated in Fig. S12b, consistent to FTIR results. In contrast, the 3.0% CaF_2@NMC811 sample still exhibits a distinct carbonate signature peak after water exposure, as shown in Fig. S13b, signifying that the majority of the original Li_2CO_3 remains embedded under the CaF_2 coating,
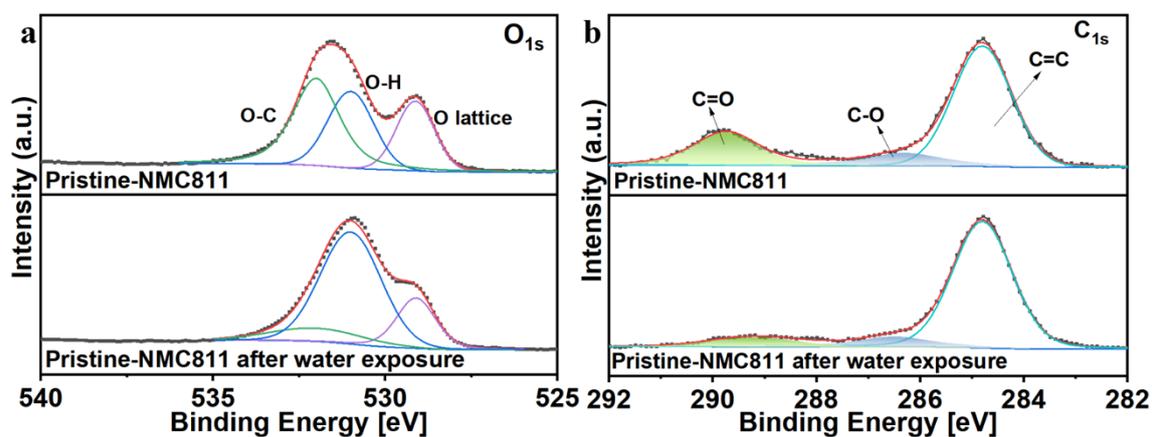
making it impervious to removal by water.

Fig. S12. XPS spectra of the pristine-NMC811 samples before and after water exposure for (a) O 1s and (b) C 1s, respectively.
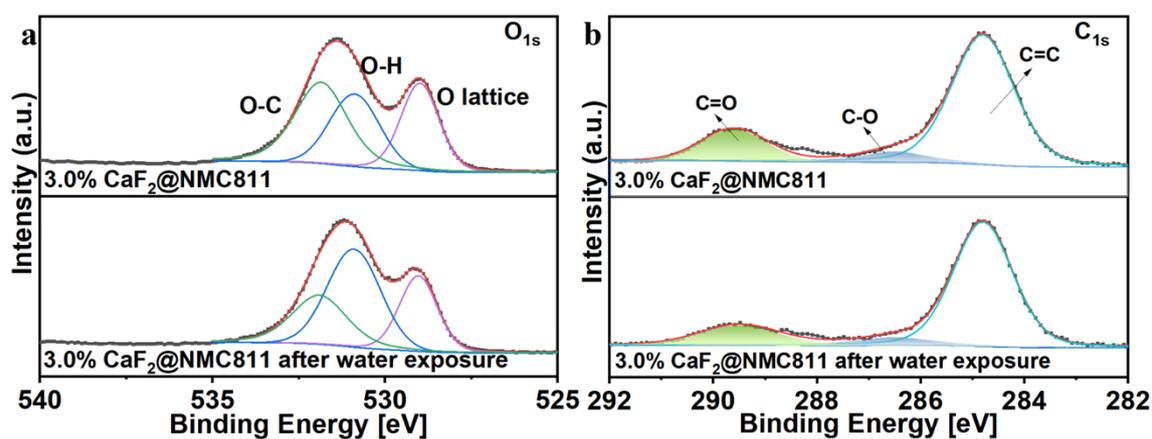

Fig. S13. XPS spectra of the 3.0% CaF$_2$@NMC811 samples before and after water exposure for (a) O 1s and (b) C 1s, respectively.
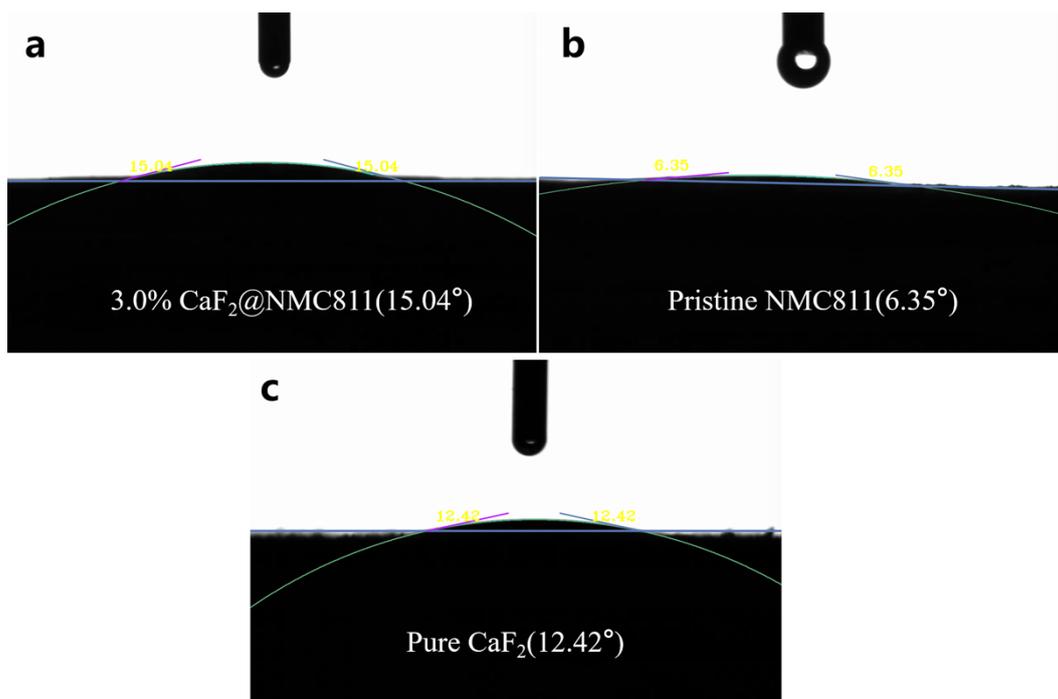
Fig. S14. Water droplets contact angle for (a) 3.0% CaF$_2$@NMC811, (b) pristine-NMC811, and (c) pure commercial CaF$_2$ powder.

Static contact angle measurement is commonly employed to study the wetting /hydrophilicity characteristics of a material's surface. The values shown in Fig. S14 are wetting angles, demonstrating NMC811 after CaF$_2$ coating shows hydrophilic property. Commercial CaF$_2$ powder also shows hydrophilic nature, consistent with previous reports.[1-3]

To demonstrate the advantages of low water soluble CaF_2, we treated NMC811 directly with NF_3 gas at the same temperature 300 °C, i.e. without the precipitation step of introducing Ca ions. The obtained sample is indexed as NF_3@NMC811. Without the bonding of Ca ions, the coating can be easily washed off, see Figure S15, F1s signal completely disappeared after water exposure opposed to CaF_2 coated sample, in which Ca 2p signals and F 1s signal slightly dropped. The Ni 2p spectrum of NF_3@NMC811 reveals that the Ni^{3+} percentage drops from 87.53% to 78.02% after exposure. This drop signifies a degree of active nickel being reduced to the divalent state, indicating the water-soluble coating cannot protect NMC811 from water erosion.
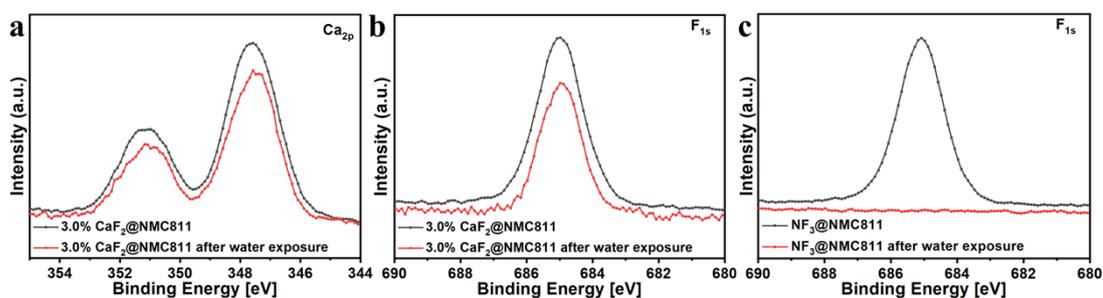

Fig. S15. XPS spectra of the 3.0% CaF_2@NMC811 sample before and after water exposure for (a) Ca 2p and (b) F 1s, respectively, and F 1s XPS spectrum of NF_3@NMC811 sample before and after water exposure.
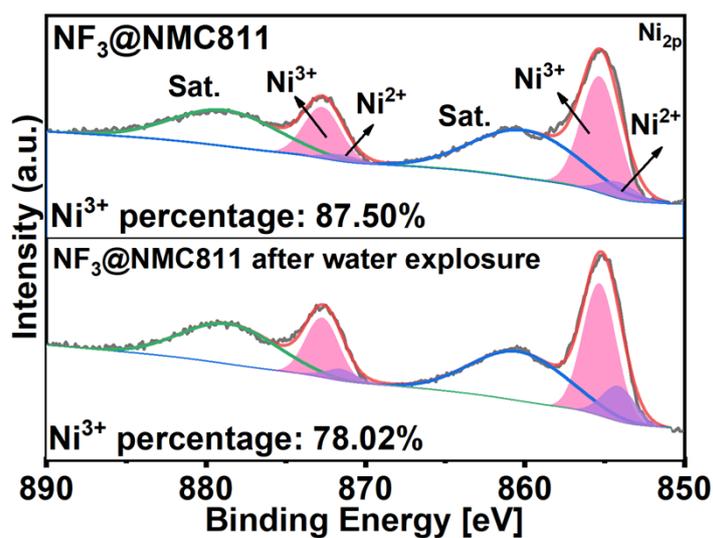
Fig. S16. Ni 2p XPS spectra of the NF$_3$@NMC811 sample before and after water exposure.

The XRD result, Figure S17 also demonstrates that due to higher solubility of coating on NF$_3$@NMC811, Li$^+$/H$^+$ exchange happened during water exposure, resulting in cation mixing. The (003)/(104) ratio decreased to 1.02, which strongly indicates structural transformation within the material after water exposure.

Fig. S17. XRD pattern of NF$_3$@NMC811 after water exposure.

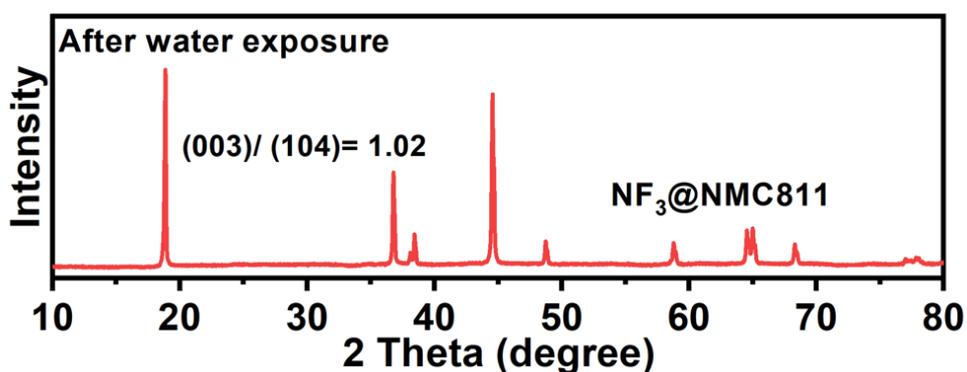The pH of the water after rinsing with NF$_3$@NMC811 was 9.5, compared to 6.6 of deionized water, 12.3 of water rinsing with pristine NMC811 and 7.1 of water rinsing with 3.0% CaF$_2$@NMC811, further confirming the coating with low water solubility is key to protect NMC811 from Li$^+$/H$^+$ exchange in water.

Relationships between solubility, hydrophilicity and hydrophobicity, and the role of CaF$_2$ in micro and macro perspectives

Dissolving a material in water usually involves several steps. Firstly, solid materials are broken apart into individual molecules or ions, often requiring energy input to overcome intermolecular or ion bonding forces. Subsequently, interactions between solute molecules or ions and water molecules lead to hydration, forming dissolved species in the solution. Additionally, the process involves diffusion, where solute molecules or ions leave the solid crystal and diffuse into the solution, as well as interactions with other solvent molecules (e.g., hydrogen bonding, etc.).

Hydrophobicity and hydrophilicity, according to their original meanings in Greek, pertain to the affinity with water. One of the measures of hydrophilicity and hydrophobicity is the free energy of hydration (van Oss, C. J. Interfacial Forces in Aqueous Media; Marcel Dekker, Inc.: New York, 1994).

The interaction between solute molecules or ions and water molecules during dissolving is indeed related to their affinity for water. This affinity determines how strongly the solute molecules or ions are attracted to the water molecules, influencing the dissolution process. High affinity for water (hydrophilic) favors interacting with water molecules and dissolving readily, whereas low affinity for water (hydrophobic) means not interacting strongly with water molecules and probably remaining insoluble or poorly soluble.

However, the dissolution process is not only determined by the affinity for water. While hydrophobicity does contribute to insolubility, other factors may be at play. For instance, a material might be insoluble in water due to its molecular/crystal structure or because it forms strong bonds with itself that are not easily broken by water molecules. Therefore, insolubility in water does not necessarily imply that a material is hydrophobic.

Conversely, there are also several factors influencing surface's hydrophilicity or hydrophobicity, which determine its affinity for water, e.g. chemical composition, surface energy, surface microstructure and surface charge, etc. Chemical composition is one of determining factors.

Therefore, a material is not insoluble in water, it is not necessarily hydrophobic. This principle applies equally to the surface composed of this material.

CaF_2 is considered hydrophobic, which is because the bond between Ca^{2+} and F^- in CaF_2 is very strong, making it difficult for water molecules to break into the structure and thus not possible to interact with the ions. It, in many cases, exhibits hydrophilic characteristic[1-3], depending on its crystallographic surface, form and lattice purity, etc.

Here, it also presents hydrophilic, evidenced by Figure S14. The contact angle measurements for all the samples, including pure commercial CaF_2 and 3.0% CaF_2 protected NMC811, do display small wetting angles, which is probably due to the strong H-bonding interaction between CaF_2 and water[2].

In the context of interfacial instability observed in nickel-rich layered cathode materials in humid environment, the exchange of Li^+ and H^+ ions serve as the primary mechanism behind moisture erosion. This phenomenon suggests that the bonding of Li^+ within the structure is comparatively feeble; indeed, were this not the case, the

electrochemical deintercalation of lithium ions from the NMC811 structure would be unattainable. Conversely, the bonding between Ca^{2+} and F^- ions within the coating layer is robust enough, effectively inhibiting H^+ ions/water molecules to break through the layer, thus impeding the occurrence of Li^+/H^+ exchange. From a macroscopic perspective, the CaF_2 layer exhibits low water soluble. Therefore, the ability for cathode materials to resist water erosion is not inherently linked to either hydrophobicity or hydrophilicity, but lies in robust chemical bonding within the protective layer, which, on a macroscopic scale, exhibits low water solubility.

1. Zhang X., Wang X. M., Miller J. D., Surf. Innov. 2015, 3(1), 39-48.

2. Kim D., Kim E., Park S., Kim S., Min K. B., Yoon J. H., Kwak K., Cho M., Chem 2021, 7, 1602–1614.

3. Chevalier N. R., RSC Adv., 2017, 7, 45335.